

## Adsorption of CH<sub>3</sub>OH, H<sub>2</sub>O, CO, H<sub>2</sub>, CO<sub>2</sub> over zinc oxide surfaces

João B. L. Martins<sup>1</sup>(PQ), Italo P. de Lima<sup>1</sup>(PG), Elton A. S. de Castro<sup>2</sup>(PQ), Ricardo Gargano<sup>3</sup>(PQ)

1. Instituto de Química, Universidade de Brasília, Brasília, DF, CP 4478, 70904970, Brazil

2. UEG, Av. Universitária s/n, Formosa, GO, 73807-250, Brazil.

3. Instituto de Física, Universidade de Brasília, DF, CP 4455, 70919970, Brazil.

Keywords: Adsorption, ZnO, ONIOM, Plane Wave.

### 1. INTRODUCTION

There is a considerable interest in understanding the interaction of molecules on metal oxide surfaces. The role of adsorption on metal oxides is central in many technological areas such as gas sensors and heterogeneous catalysis. Metal oxide systems are of fundamental importance in many applications going from electronic devices to heterogeneous catalysis. Moreover the interfaces between the deposited metal and metal oxide play a prominent part in the subsequent properties of the metal/oxide system. Experimental spectroscopic studies of bulk metal oxides are limited due in part to the low conductivity of oxides [1] and phonon loss.

Zinc oxide is a major component of Cu/ZnO based catalysts which are highly effective for the methanol synthesis from CO/H<sub>2</sub> and CO<sub>2</sub>/H<sub>2</sub> mixtures [2-4]. Pretreatment with CO/H<sub>2</sub> mixture caused a transient increase of the methanol formation. Methoxide species was formed in the course of the pretreatment, being readily hydrolysed by water formed via the reverse water gas shift reaction [2]. Methanol synthesis on ZnO catalysts must be run under severe conditions of 573-673K under 150-200 atm of reaction gases to achieve significant activity. The synthesis with the copper promoted, Cu/ZnO, is active at 473-523K and used industrially at pressures of 50-100 atm [5]. The activation barrier for the methanol synthesis is only 18 kcal/mol with the Cu/ZnO as compared to almost 30 kcal/mol on ZnO [6]. The geometric configurations that HCOO(adsorbed) adopts on oxide surfaces are substrate dependent. A monodentate type structure has been suggested for HCOO(a) adsorbed on ZnO (0001) Zn terminated, in which a single O atom bonds to the metal center. HCOO(a) adopts a bidentate and monodentate type structure on the (10 $\bar{1}$ 0) and

(000 $\bar{1}$ )O terminated surfaces, respectively [7,8]. The bidentate structure was also assigned to the formic acid on Cu(110).

No dissociative adsorption on (10 $\bar{1}$ 0) ZnO surface was suggested from UPS spectra [9]. Methanol adsorption on ZnO (0001) polar faces studies shows a formation of methoxy species at low temperature [10]. The UDP and TDS experiments indicate molecular adsorption of methanol on ZnO surface at low temperatures [10].

The role of the ZnO and Cu in Cu/ZnO based catalysts is still controversial. There are two main groups regarding the methanol formation site: methanol is formed on a metallic Cu surface and other for which occurs an active sites [11] on the ZnO surface due to substitutional Cu ion. Fujitani and Nakamura [11] have studied the surface science data for the Cu/ZnO system and proposed an active site model in which Zn species present on the Cu surface promote the methanol synthesis. CO chemisorbs to the Cu promoted catalyst more strongly than to either Cu or ZnO [12-13]. Didziulis and co-workers [12] studied the CO adsorption on Cu/ZnO system, they found the formation of copper monolayers on ZnO surfaces (0001) (000 $\bar{1}$ ) and (10 $\bar{1}$ 0). Copper on is much reactive on 0001 surfaces, and less reactive on (000 $\bar{1}$ ) surface, while copper on the (10 $\bar{1}$ 0) shows intermediate reactivity. The CO chemisorbs on (0001) and (10 $\bar{1}$ 0) surface with approximately the same affinity as copper metal ( $\Delta H_{ads}$ =15-16 kcal/mol), while chemisorption on Cu/ZnO 000-1 was much weaker ( $\Delta H_{ads}$  < 12 kcal/mol). High affinity for CO chemisorption was also obtained ( $\Delta H_{ads}$ = 21 kcal/mol). The CO<sub>2</sub> hydrogenation reaction is structure sensitive, the copper (111) face is active while the (110) crystal face is less so [14]. Hydrogenation of the formate reaction intermediate that forms from CO<sub>2</sub> is thought to be

the rate-determining step to produce methanol. Methanol synthesis activity on Cu from CO<sub>2</sub>/H<sub>2</sub> is structure sensitive [15].

The adsorption of CO<sub>2</sub> on polar (0001) surface was scarcely investigated. On the (0001) surface, each zinc cation has a single vacant coordination in relation to the bulk within oxygen anions. This is the requirement for the dissociation of Brønsted acids on acid and basic site pairs of ZnO surfaces [16]. A molecular beam study of CO<sub>2</sub> on (0001) surface showed an adsorption heat of 34 kJ.mol<sup>-1</sup> [17-19] in agreement to the physisorption heat of 31 kJ.mol<sup>-1</sup>, while chemisorption of 140 kJ.mol<sup>-1</sup> was reported for the nonpolar surface [20-21]. C K-edge near edge X-ray absorption fine structure presents a peak at 290eV for the (0001) surface and an angle of 68° between surface normal and molecular plane [22]. Low-energy electron diffraction (LEED) analysis showed that CO<sub>2</sub> adsorbs with both carbon and oxygen on (0001) surface [23].

The activity of the Cu/ZnO catalyst is affected by strong synergistic interactions between the Cu and ZnO components [24]. Cu<sup>+</sup> and metallic Cu have been postulated as the active species for the methanol synthesis [24]. In the case of the water-gas shift reaction, it is known that metallic Cu supported on ZnO is the active catalytic species [24]. X-ray photoelectron diffraction indicates that metals are disordered with respect to substrate sites at submonolayer coverages [25]. The evidence here is that subcritical coverages induce no new fine structure in the scans of substrate XPS intensity vs. angle, for Cu/ZnO(0001̄)-O [25]. All experimental results suggest that Cu is rather metallic [25].

It is known that the activity of the Cu/ZnO system is much greater than the combined activities of the separate components [26-27]. According to the mechanism proposed by Kinnaird and co-workers Cu-formates (HCOO<sup>-</sup>) are important for the methanol formation [26-27].

The effect of support on methanol synthesis was studied by Burch et al. [26-27]. Cu catalysts are strongly dependent on which oxides are present. ZnO is a much better promoter than SiO<sub>2</sub>. The physical mixture of Cu/ZnO exhibits high relative activity compared to the Cu alone [26-27]. Cu methanoates are more readily created if the surface is only partly reduced. [26-27]. They indicate that the rate-determining step in methanol synthesis occurs on the Cu but that this step is accelerated in the presence of even small amounts of ZnO [26-27]. Millar et al. have also

proposed that interfacial formate species located at the boundary between copper and zinc oxide may also play a minor role in the industrial reaction [28].

The LDA results of Casarin and co-workers using saturated clusters of (ZnO)<sub>14</sub> and (ZnO)<sub>24</sub> include a surface relaxation, clean and doped Cu/ZnO system: Jaffe and co-workers have done a periodic HF calculation of ZnO (1010) surface relaxation optimizing four coordinate parameters [29]. Martins and co-workers [30] using AM1 semi-empirical method have optimized the cluster structure. The theoretical results of surface relaxation are in good agreement with experimental data.

The DFT [31-32], AM1 [33] and *ab initio* [33] results for the CO adsorption on the ZnO(10-10) show an increase in C-O bond length in agreement with the experimental studies.

The aim of this work is to study the methanol formation, catalyzed by ZnO. The *ab initio* and semi-empirical methods are employed. The geometry of different intermediates for methanol formation from the CO/H<sub>2</sub>/CO<sub>2</sub> formation is optimized throughout semi-empirical AM1 method. The *ab initio* method is used in order to calculate structure energies, orbital SCF energies and Mulliken charge.

## 2. METHOD AND MODELS

ZnO crystallizes in a structure of B4 type (wurtzite) of P<sub>6</sub>mc space group [34]. The experimental lattice parameters values are *a*=3.2495 Å and *c*=5.2069 Å, and the internal parameter is *z* = 0.3825 Å [35]. DFT has been largely used to describe the adsorption on surfaces of metal oxides, specifically the structural and electronic properties. Bulk parameters of ZnO were well established using DFT and pseudopotentials [36-37]. The DFT calculations were performed using the Gaussian 03 package. The 3-21G basis set level was used for Zn, O, C and H atoms. The cluster model has shown reasonable results when used to investigate the adsorption of CO, H<sub>2</sub> and water on ZnO surfaces [33,38]. Cluster models are reliable tools to study surfaces and adsorption due to its simplicity. However in order to take into account the Madelung potential and avoid dangling bonds there are two ways used in the non-periodic calculations: i) embedding the cluster in a point

charge [39] or ii) using saturators [31]. We have used the embedded method. The  $(\text{ZnO})_{16}$  cluster model was embedded in a PC of 736 points (Figure 1). The charge was optimized in order to minimize the ionicity effect.

Periodic calculations were performed using DFT. PBE and PW91 functionals gives almost the same mean errors for bond lengths, and the best-performing exchange-correlation potentials are found to be Becke–Perdew, PBE and PW91, while all electron PBE and PW91 adsorption energies and structures give the same trend and almost the same results for CO adsorption. Therefore, the exchange and correlation effects were obtained according to the generalized gradient approximation (GGA) using the PW91 functional implemented in the algorithm of VASP4.6 computational code. The O  $2s^2 2p^4$ , Zn  $3d^{10} 2s^2$ , and C  $2s^2 2p^2$  were treated as valence states. The atomic positions of  $\text{CO}_2$  molecule and ZnO were relaxed with full optimization using the Quasi-Newton algorithm. The energy cutoff was 420 eV, and the K points mesh was  $3 \times 3 \times 3$  in the first Brillouin zone. All forces were converged with criteria less than  $0.20 \text{ eV}/\text{\AA}$  per atom. The positions of the nuclei were relaxed using ultrasoft pseudopotential (US-PP) method to describe the ion-electron interaction with eigenstates expanded in basis functions like plane waves, while PAW method was used for property analysis.

In this work we have studied *slabs* of ZnO of four, six and eight layers (Figure 1) with  $(\text{ZnO})_{32}$ ,  $(\text{ZnO})_{48}$  and  $(\text{ZnO})_{64}$  units, respectively. The overlayer structures on (0001) and  $(000\bar{1})$  surfaces for the adsorbed molecules were described using Wood's notation of  $(2 \times 2)$  surface. The adsorbate coverage was  $\theta = 1/8$  for these structures. The (0001) surface area was  $74.94 \text{ \AA}^2$  for all supercell *slabs*. This value was chosen in order to minimize the dipole moment of the *slab*. It was also used a vacuum of  $10 \text{ \AA}$  along the  $z$  axis.

Another point of interest of this work was to analyze the adsorbed molecule by means of total and partial densities of electronic states (DOS). We have evaluated the energies of physical and chemical adsorptions, valence bands, *band gap*, states, and final filled states due to atomic displacements. Electron localization function (ELF) analysis was performed using the DGRID program.

### 3. RESULTS AND DISCUSSION

Table 1 shows the results for the cluster model. The interaction distances are closer to the Zn-O distance of  $2.1 \text{ \AA}$ . CO interaction energy is closer to the experimental values [40].  $\text{CO}_2$  has the largest interaction energy, while hydrogen has the weakest interaction; this trend is in accordance to the experimental results. The hydrogen bonding groups of  $\text{H}_2\text{O}$  and  $\text{CH}_3\text{OH}$  have the same interaction with ZnO.

Table 1 – Cluster model results using ONIOM method (B3LYP:UFF). Distance is in ( $\text{\AA}$ ) and Interaction Energy (IE) is in  $\text{kJ}\cdot\text{mol}^{-1}$ .

|                  | $\text{CH}_3\text{OH}$ | $\text{H}_2\text{O}$ | CO   | $\text{H}_2$ | $\text{CO}_2$ |
|------------------|------------------------|----------------------|------|--------------|---------------|
| dC-Zn            | 3.44                   | 2.08                 | 2.28 | -            | 2.58          |
| dO-Zn            | 2.09                   | -                    | 3.39 | -            | -             |
| dO- $\text{O}_s$ | -                      | 2.46                 | 3.24 | -            | -             |
| dC-H             | 1.09                   | 0.97                 |      | -            | -             |
| dO-H             | 1.01                   | 1.03                 |      | -            | -             |
| dC- $\text{O}_s$ | -                      | -                    | 2.62 | -            | 1.53          |
| dC-O             | 1.46                   | -                    | -    | -            | 1.24/<br>1.30 |
| dH-Zn            | -                      | -                    | -    | 2.62         | -             |
| dH- $\text{O}_s$ | -                      | -                    | -    | 3.33         | -             |
| IE               | -145                   | -151                 | -61  | -7           | -239          |

Plane wave adsorption energy of  $\text{CO}_2$  bidentate specie is  $407.8 \text{ kJ}\cdot\text{mol}^{-1}$ . This value is smaller than those obtained by Martins and co-workers using semiempirical AM1, and *ab initio* Hartree-Fock method with 3-21G\* basis set (RHF/3-21G//AM1) with cluster models [41]. One main advantage of using plane wave basis set is in relation to the basis set superposition error (BSSE), which must be accounted for the LCAO based methods. The results for cluster models have no implicit periodicity, while the importance of periodic conditions is clear for such solid systems. Therefore, it was expected that periodic plane wave results were in better agreement to experimental data.

ELF analysis for the chemical adsorption with bidentate and tridentate species (Figure 1) indicates a covalent bonding between  $\text{CO}_2$  and the (0001) surface in both adsorptions. In contrast to the physical adsorption, ELF shows a clear interaction between the  $\text{CO}_2$  molecule and the surface for chemical adsorption.

Table 2: Comparison between the theoretical results of adsorption energy of CO<sub>2</sub> with tridentate using periodic plane wave method.

|   | This work | Ref. [3]* |
|---|-----------|-----------|
| E <sub>ads</sub> (kJ/mol)                             | -396.9    | -55.0     |
| O - Zn <sub>2</sub> (Å)                               | 2.02      | 2.07      |
| O - Zn <sub>3</sub> (Å)                               | 2.03      | 2.07      |
| C - Zn (Å)  | 2.06      | 2.06      |
| C <sub>CO<sub>2</sub></sub> -Zn <sub>(0001)</sub> (Å) | 1.52      | 1.41      |
| O <sub>CO<sub>2</sub></sub> -Zn <sub>(0001)</sub> (Å) | 1.85      | 1.89      |
| O <sub>CO<sub>2</sub></sub> -Zn <sub>(0001)</sub> (Å) | 1.85      | 1.89      |

\*The geometrical parameters and adsorption energy were reported for the (2x2) unit cell.

Table 2 shows a comparison between adsorption of CO<sub>2</sub> tridentate specie of the current study and the results of atom-centered basis set of Chuasiripattana on ZnO (0001) surface [3], with adsorption energy in the borderline of physical adsorption. The interatomic distances of this work are in agreement to the reported (2x2) supercell [3]. However, the results for adsorption energies are not in agreement with the previous theoretical study of (2x2) unit cell [3]. At low coverage (1/9ML), the adsorption energy calculated in a (3x3) unit cell is 108.1kJ.mol<sup>-1</sup> [3]. Heat of adsorption for the tridentate specie on oxygen terminated (000 $\bar{1}$ ) surface was calculated to be 139 kJ.mol<sup>-1</sup> using PBE functional with cluster model [4].

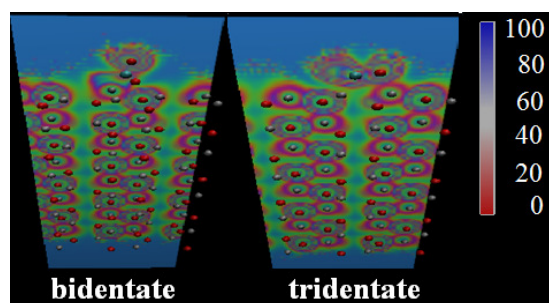


Figure 1 – Bidentate and tridentate adsorbed species using plane wave method.

Carbon dioxide is held on zinc oxide with energies from 108.8 to 154.8 kJ.mol<sup>-1</sup> [42]. The experimental heat of adsorption for the pristine sites amounts to 34.0 kJ/mol for

the (0001) surface [18]. This is slightly larger than the value reported for the physisorption of CO<sub>2</sub> of 31 kJ.mol<sup>-1</sup> by Goepel et al. [20]. Heats of adsorption of 140 kJmol<sup>-1</sup> for CO<sub>2</sub> chemisorption has been reported on nonpolar ZnO surfaces [20]. Chuasiripattana and co-workers [3] have used a numerical atom-centered basis set with PBE, with lattice parameters of a=3.302 Å and c=5.317 Å larger than experimental values, while we have used PW91. It is well known that these functionals leads to the difference in interaction energies. Therefore, this difference is partially due to exchange correlation functional and the number of layers used, since there is no significant difference of our structure in relation the reported data [3].

#### 4. Conclusions

In this work we carried out interaction surfaces of ZnO using cluster, US-PP and PAW methods. We investigated the structural and electronic properties of physical and chemical adsorption with focus on adsorption energies, and defined the minimum number of layers needed for the adsorption study. The atom positions were fully relaxed. The surface energy suggests that the slab with more than four layers were needed to study the adsorption process. Our results are in agreement with experiments using X-ray photoelectron spectroscopy that investigated the physical adsorption, and found states filled by CO<sub>2</sub> in the lower energy regions. One main advantage of using plane wave basis set is in relation to the BSSE. In addition, comparing our chemical adsorption results with cluster models show the importance of periodic conditions for such solid systems. ELF for the chemical adsorption with bidentate and tridentate showed a clear interaction between the CO<sub>2</sub> molecule and the surface.

Acknowledgements: CNPq, FAPDF, UnB and CAPES.

#### 3- REFERENCES:

1. G. Thornton, S. Crook, Z. Chang, *Surf. Sci.* 415, 122 (1998).
2. S. I. Fujita, H. Ito, N. Takezawa, *Bull. Chem. Soc. Jpn.* 66, 3094 (1993).
3. K. Chuasiripattana, O. Warschkow, B. Delley, C. Stampfl, *Surf. Sci.* 604, 1742 (2010).
4. J. Kossmann, G. Rossmuller, C. Hattig, *J. Chem. Phys.* 136, 034706 (2012).
5. Y. Borodko, G. A. Somorjai, *Appl. Catal. A-Gen* 186, 355 (1999).
6. A. Steinfeld, C. Larson, R. Palumbo, M. Foley, *Energy* 21, 205 (1996).
7. S. Crook, H. Dhariwal, G. Thornton, *Surf. Sci.* 382, 19 (1997).
8. W. T. Petrie, J. M. Vohs, *Surf. Sci.* 245, 315 (1991).
9. G. W. Rubloff, H. Lüth, W. D. Grobman, *Chem. Phys. Lett.* 39, 493 (1976).
10. W. Hirschwald, D. Hofmann, *Surf. Sci.* 140, 415 (1984).
11. T. Fujitani, J. Nakamura, *Appl. Catal. A* 191, 111 (2000).
12. S. V. Didziulis, K. D. Butcher, S. L. Cohen, E. I. Solomon, *J. Am. Chem. Soc.* 111 (1989).
13. R. G. Herman, K. Klier, G. W. Simmons, B. P. Finn, J. B. Bulko, *J. Catal.* 56, 497 (1979).
14. B. Sakakini, J. Tabatabaei, M. J. Watson, K. C. Waugh, F. W. Zeicael, 105, 369 (1996).
15. K. C. Waugh, *Catal. Lett.* 58, 163 (1999).
16. M. A. Barteau, *J Vac Sci Technol A* 11, 2162 (1993).
17. J. Wang, U. Burghaus, *J. Chem. Phys.* 123 (2005).
18. J. Wang, U. Burghaus, *Chem. Phys. Lett.* 403, 42 (2005).
19. J. Wang, U. Burghaus, *J. Chem. Phys.* 122 (2005).
20. W. Göpel, R. S. Bauer, G. Hansson, *Surf. Sci.* 99, 138 (1980).
21. W. Hotan, W. Göpel, R. Haul, *Surf. Sci.*, 83, 162 (1979).
22. A. Gutierrez-Sosa, T. M. Evans, S. C. Parker, C. T. Campbell, G. Thornton, *Surf. Sci.* 497, 239 (2002).
23. W. H. Cheng, H. H. Kung, *Surf. Sci.*, 122, 21 (1982).
24. S. Chaturvedi, J. A. Rodriguez, J. Hrbek, *J. Phys. Chem. B* 101, 10860 (1997).
25. C. T. Campbell, *J. Chem. Soc., Faraday Trans.* 92, 1435 (1996).
26. R. Burch, R. J. Chappell, S. E. Golunski, *J. Chem. Soc., Faraday Trans. I* 85, 3569 (1989).
27. R. Burch, S. E. Golunski, M. S. Spencer, 86, 2683 (1990).
28. G. J. Millar, I. H. Holm, P. J. R. Uwins, *J. Drennan*, 94, 593 (1998).
29. J. E. Jaffe, N. M. Harrison, A. C. Hess, *Phys. Rev. B-Condens Matter* 49, 11153 (1994).
30. J. B. L. Martins, E. Longo, J. Andres, *Int. J. Quantum Chem.:Quantum Chem. Symposium* 27, 643 (1993).
31. M. Casarin, C. Maccato, A. Vittadini, *Appl. Surf. Sci.* 142, 192 (1999).
32. M. Casarin, C. Maccato, A. Vittadini, *Inorg. Chem.* 37, 5482 (1998).
33. J. B. L. Martins, E. Longo, J. G. R. Tostes, C. A. Taft, J. Andres, *Theochem-J. Mol. Struct.* 109, 19 (1994).
34. S. C. Abrahams, J. L. Bernstein, *Acta Cryst. B* 25, 1233 (1969).
35. I. R. Shein, V. S. Kiiko, Y. N. Makurin, M. A. Gorbunova, A. L. Ivanovskii, *Phys. Solid State* 49, 1067 (2007).
36. F. Y. Zhang (2011), *Physica B* 406, 3942 (2011).
37. Z. Charifi, H. Baaziz, A. H. Reshak, *Phys Status Solidi B-Basic Solid State Phys* 244, 3154 (2007).
38. J. B. L. Martins, E. Longo, J. Andres, C. A. Taft, *Theochem-J. Mol. Struct.* 335, 167 (1995).
39. M. Yoshimoto, S. Takagi, Y. Umemura, M. Hada, H. Nakatsuji, *J. Catal.* 173, 53 (1998).
40. E. I. Solomon, P. M. Jones, J. A. May, *Chem. Rev.* 93, 2623 (1993).
41. J. B. L. Martins, E. Longo, O. D. R. Salmon, V. A. A. Espinoza, C.A. Taft, *Chem. Phys. Lett.* 400, 481 (2004).
42. M. Bowker, H. Houghton, K. C. Waugh, *J Chem Soc, Faraday Trans I* 77, 3023 (1981).